Journal of Medicinal Chemistry

Article

Synthesis and Characterization of Fluorine-18 labeled N-(4-Chloro-3-((fluoromethyl-d2)thio)phenyl)picolinamide for Imaging of mGluR4 in Brain

Junfeng Wang, Xiying Qu, Timothy M. Shoup, Gengyang Yuan, Sepideh Afshar, Chuzhi Pan, Aijun Zhu, Ji-Kyung Choi, Hye Jin Kang, Pekka Poutiainen, Georges ElFakhri, Zhaoda Zhang, and Anna-Liisa Brownell

J. Med. Chem., **Just Accepted Manuscript** • DOI: 10.1021/acs.jmedchem.0c00201 • Publication Date (Web): 21 Feb 2020

Just Accepted

is published by the American Chemical Society. 1155 Sixteenth Street N.W., Washington, DC 20036

Synthesis and Characterization of Fluorine-18 labeled *N*-(4-Chloro-3-((fluoromethyl-d_2)thio)phenyl)picolinamide for Imaging of mGluR4 in Brain

Junfeng Wang,[1&] Xiying Qu,[1&] Timothy M. Shoup,[1&] Gengyang Yuan,[1] Sepideh Afshar,[1] Chuzhi Pan,[1,2] Aijun Zhu,[1] Ji-Kyung Choi,[3] Hye Jin Kang,[4] Pekka Poutiainen,[5] Georges ElFakhri,[1] Zhaoda Zhang[3]* and Anna-Liisa Brownell[1]*

[1]Gordon Center for Medical Imaging, Massachusetts General Hospital and Harvard Medical School, 125 Nashua Street, Suite 660, Boston, MA 02114

[2]The Third Affiliated Hospital of Sun Yat-sen University, 510630, China

[3]Athinoula A. Martinos Center for Biomedical Imaging, Massachusetts General Hospital and Harvard Medical School, 149 Thirteenth Street, Suite 2301 Charlestown, MA 02129

[4]Department of Pharmacology, University of North Carolina Chapel Hill School of Medicine, Chapel Hill, North Carolina 27514, United States

[5]University Central Hospital of Kuopio, 70210 Kuopio, Finland

& Equal contribution

ABSTRACT

We have synthesized and characterized [^{18}F]-*N*-(4-chloro-3-((fluoromethyl-d_2)thio)phenyl)-picolinamide ([^{18}F]**15**) as a potential ligand for the PET imaging of mGluR4 in the brain. Radioligand [^{18}F]**15** displays CNS drug-like properties, including mGluR4 affinity, potent mGluR4 PAM activity and selectivity against other mGluRs, as well as sufficient metabolic stability. Radiosynthesis was carried out in two steps. The radiochemical yield of [^{18}F]**15** was 11.6 ± 2.9% (n = 7, decay corrected) with a purity of 99% and a molar activity of 84.1 ± 11.8 GBq/µmol. *Ex vivo* biodistribution studies showed reversible binding of [^{18}F]**15** in all investigated tissues including the brain, liver, heart, lungs, and kidneys. PET imaging studies in male Sprague-Dawley rats showed that [^{18}F]**15** accumulates in the brain regions known to express mGluR4. Pretreatment with the unlabeled mGluR4 PAM compounds **13** (methylthio analog) and **15** showed significant dose-dependent blocking effects. These results suggest that [^{18}F]**15** is a promising radioligand for PET imaging mGluR4 in the brain.

INTRODUCTION

Parkinson's disease (PD) is the second most common neurodegenerative disorder affecting more than six million people worldwide.[1-2] PD results from the progressive loss of dopaminergic neurons in the Substantia Nigra pars compacta (SNpc), causing dysfunction of the basal ganglia (BG) motor circuit.[3-4] The current pharmacotherapy aims to replace missing dopamine by using the dopamine precursor levodopa (L-DOPA). This treatment provides symptomatic relief and is successful in the early PD medication period,[5] however, as the disease progresses L-DOPA becomes less effective and produces debilitating side effects such as L-dopa-induced dyskinesia (LID).[6-7] Hence the development of a disease modifying therapy for PD remains a challenge for researchers.

Over the last decade, metabotropic glutamate receptor 4 (mGluR4) has gained interest due to the potential benefits in treating numerous neuronal diseases such as PD, LID and other disorders.[6, 8-9] The mGluR4 receptor is expressed at multiple synapses in desired regions of the BG motor circuit, mainly localized presynaptically in the striatum, hippocampus, thalamus, and cerebellum.[10-12] As a group III mGluR, mGluR4 interacts with the $G_{ai/o}$ subunit of G-protein that negatively couples with adenylate cyclase to inhibit cAMP dependent signal pathways.[1, 13] Its activation reduces presynaptic neurotransmitter release, subsequently, decreasing output of the indirect pathway. This is a promising strategy to normalize the BG circuitry in PD and ultimately reduce or eliminate PD symptoms.[3, 5, 8, 10] Consequently, this approach has opened a new avenue for developing nondopaminergic treatments for PD and for identifying novel disease modifying therapeutics.

As a family C GPCR, the activation of mGluR4 can be accomplished or enhanced by two different mechanisms: orthosteric agonists or positive allosteric modulators (PAMs). Although most orthosteric ligands lack clear subtype-selectivity and/or blood–brain barrier (BBB) penetration, few examples of selective and brain penetrant orthosteric agonists such as LSP4-2022 have been reported.[14-15] Since allosteric modulators may offer some benefits such as subtype-selectivity, retained physiology of the receptor and the saturation effects, substantial effort has been focused on development of mGluR4 PAMs as new therapeutics for neurological diseases such as PD and LID.[6] Hundreds of mGluR4 PAMs have been reported and/or patented since 2009.[16-17] Figure 1 shows some representative mGluR4 PAMs, of which compounds **1-10** have demonstrated antiparkinsonian activity in animal models of PD.[18-28] Compound **11** is a potent mGluR4 PAM that has been used as the reference compound for mGluR4 PAM activity.[28] Prexton Therapeutics (Prexton) announced in 2017 the launch of phase II clinical trial of its investigational drug candidate, PXT002331 (**10**, Foliglurax), in PD.[6]

[Figure 1]

An efficient PET radioligand for mGluR4 could be an important tool for understanding the role of mGluR4 in healthy and disease conditions, and also for the development of new drugs targeting this receptor.[9, 29] PET offers picomolar sensitivity and is a fully translational technique; therefore, extensive research efforts have been directed towards the development of PET ligands suitable for *in vivo* probing of mGluR4 (Figure 2).[30-33] In the past, we have studied the pharmacokinetics of [^{11}C]**4,** ([^{11}C]ML-128), [^{18}F]**12** ([^{18}F]KALB001), [^{11}C]**13** ([^{11}C]mG4P012 or [^{11}C]KALB012) and [^{11}C]**14** by using PET imaging in rats. PET studies with [^{18}F]**12** and [^{11}C]**13** were conducted also in non-human primates.[31] These PET radiotracers have been designed and/or

developed based on mGluR4 PAMs.

[Figure 2]

Among these PET ligands, the *in vitro* data revealed that compound **13** has sufficient mGluR4 binding affinity and selectivity over other mGluRs, as well as a suitable metabolic stability.[32] PET studies in rats showed that [^{11}C]**13** accumulated rapidly into the brain and had higher uptake, slower washout and 25% better contrast than [^{11}C]**4**, indicating improved imaging characteristics as a PET radiotracer for mGluR4.[32] The improved pharmacological properties and the enhanced imaging characteristics indicated that [^{11}C]**13** is a useful PET radiotracer for mGluR4 in biological research and drug development.

Recently [^{11}C]**13** (renamed [^{11}C]PXT012253 by Prexton Therapeutics) has been used as a biomarker during the preclinical development of a potential therapeutic drug, PXT0002331 (**10**, an mGluR4 PAM), for PD and LID.[34-35] The radiotracer [^{11}C]**13** was reported to display binding in mGluR4-expressing regions in the brain of cynomolgus monkeys. Competition of [^{11}C]**13** with **10** showed high specific binding in the total distribution volume, which is useful for target occupancy or longitudinal studies. This data further supports [^{11}C]**13** as a promising PET radioligand for mGluR4 in the monkey brain and for further development in human subjects.

Development of a fluorine-18 labeled PET tracer for imaging mGluR4 is important since fluorine-18 is often the radionuclide of choice for both its physical and nuclear characteristics. Its half-life is sufficient to carry out relatively extensive imaging protocols when compared to what is possible with carbon-11. This facilitates kinetic studies and high-quality metabolic and plasma analysis, while the low positron energy associated with fluorine-18 decay leads to high imaging

resolution. We reported a fluorine-18 labeled PET tracer for mGluR4 ([^{18}F]**12**, [^{18}F]KALB001) in 2014, which showed good affinity to mGluR4 and sufficient brain uptake[31]; however, this phthalimide derivative was not stable under neutral condition and required formulation in an acidic buffer (pH 4.0). Further development of mGluR4 PET tracers indicated that [^{11}C]**13** had more favorable characteristics for imaging[32] and it initiated designing a new fluorine-18 labeled PET tracer, [^{18}F]mG4P027 ([^{18}F]**15**).

[Chart 1]

There are three possible positions to introduce fluorine-18: the 6-pyridyl, 4-chloro and 3-methylthio moieties (Chart 1). SAR results[36] indicate that 4-fluoro substitution of the chloro-atom gives reduced binding affinity which follows the order: Cl < H < F < I < Br. On the other hand, incorporation of a fluorine atom at the 6-pyrindyl position also slightly lowers the affinity and affects its metabolic stability. Next step was to evaluate the position of 3-phenyl, which is sensitive to substitutions. Our previous results showed that the 3-fluoromethoxy compound had an improved affinity compared to that of the 3-methoxy compound. Since the fluoromethylthio group may not be metabolically stable, we applied a 3-dideuteriumfluoromethylthio moiety to replace the 3-methylthio group as shown in Chart 1. Deuterium isotope effects have been used to reduce *in vivo* metabolic rates. The incorporation of dideuterium into [^{18}F]**15** could reduce the rate of defluorination initiated by cleavage of the C–H bond without altering the binding affinity to mGluR4.

Herein, we report our results on the chemical synthesis, *in vitro* pharmacochemical properties, radiolabeling, *ex vivo* biodistribution and PET imaging in rats of this new fluorine-18 labeled PET ligand for mGluR4.

RESULTS AND DISCUSSION

Chemistry. The novel unlabeled mGluR4 ligand **15** was prepared to study its *in vitro* pharmacochemical properties (Scheme 1). The reaction of methylene-d_2 bis(tosylate) **16** with cesium fluoride was carried out in *t*-amyl alcohol at 80°C to give fluoromethyl-d_2 4-methylbenzenesulfonate **17** in 48% yield. It was found that the choice of solvent used in this reaction was very important. If the reaction was carried out in acetonitrile, the yield was 5%. The thiophenol precursor **18** had been used for the radiolabeling of [^{11}C]**13**, which was prepared from 1-chloro-nitrobenzene *via* multi-steps.[32] In order to support the translational study of [^{11}C]**13**, a new synthetic route was developed for synthesis of **18** with optimized reaction conditions, resulting in an improved yield and a more efficient workup procedure.[37] The synthesis of compound **15** was achieved by treating **17** with the thiophenol precursor **18** in 92% yield.

[Scheme 1]

***In vitro* pharmacochemical properties**. To evaluate compound **15**, the pharmacochemical properties including affinity to mGluR4, mGluR4 PAM activity, selectivity to other mGluRs, lipophilicity, plasma protein binding, metabolic and solution stabilities were determined. In this study compound **15** was compared to the previously reported mGluR4 PET ligands: compounds **4**, **13** and others.

The tritium-labeled radioligand [^{3}H]**4** (*N*-(4-chloro-3-(methoxy-t_3)phenyl)picolinamide) was prepared for competitive binding assay (supporting information).[31, 38] Compounds **4**, **8**, **13** and **15** were characterized with the competitive binding assay using mGluR4 transfected CHO cells by

increasing the concentration of test compound from 0.01 nM to 10 μM in the presence of 2 nM of [^{3}H]**4**, in which the binding affinities to mGluR4 were described as IC_{50} values (Table 1).

[Table 1]

As displayed in Table 1, compound **15** has a similar IC_{50} value (3.5±0.5 nM) as that of **8** (3.2±0.6 nM) and **13** (3.5±0.7 nM) and has slightly improved affinity compared to **4** (5.1±1.1 nM). The results also confirmed that compound **15** binds to the same allosteric site of mGluR4 as that of the other three compounds.

The mGluR4 PAM activity was determined using Promega's split luciferase based GloSensor cAMP biosensor assay.[39-40] The mGluR4 PAM activity of **15** was evaluated in presence of EC_{20} concentration of agonist (1 μM L-SOP) by measuring changes in intracellular cAMP concentration, the relevant second messenger mechanism. Compound **11**, one of the most potent mGluR4 PAMs, was used as the reference compound for the assay. As shown in Figure 3, the EC_{50} values of **11** and **15** were 55 nM and 324 nM, respectively, suggesting that **15** is a moderately potent mGluR4 PAM. In the mGluR4 Gi fold shift assay, **15** shifts the agonist (L-SOP) response curves to the left 7.5-fold at 3.0 μM in 98.3% Glu Max efficacy.

[Figure 3]

The selectivity of **15** was also analyzed among the various mGluR subtypes, in which the Gq coupled receptors (mGluR1 and mGluR5) were tested using Ca^{2+} mobilization assay and the Gi/o coupled receptors (mGluR2, mGluR3, mGluR4, mGluR6 and mGluR8) using the cAMP assay.

Results demonstrated that **15** has selectivity against other mGlu receptors (Table S1) and that **15** has mGluR4 agonist activity (EC_{50} = 2.75 μM), hence, **15** is an mGluR4 ago-PAM.

Lipophilicity has a major effect on BBB penetration, ADMET properties and pharmacological activity. The values of lipophilicity (cLogP) and tPSA for **15** were calculated by using ChemDraw as 2.95 and 41.46, respectively. The $LogD_{7.4}$ of **15** was 3.82 as measured with a scaled-down shake flask method using [^{18}F]**15** (Table 2) and is in the range normally considered favorable for a PET ligand.[42]

[Table 2]

As the PET tracer is delivered into the bloodstream, it can bind to albumin, α1-acid glycoprotein and lipoproteins. Plasma protein binding (PPB) reduces the free drug in the bloodstream and inhibits BBB penetration.[42] The PPB value was obtained with an ultrafiltration assay by using [^{18}F]**15**. As Table 2 shows, the PPB of **15** was 93.1%, which gives a suitable free tracer concentration available to cross the BBB.

After iv injection PET tracers encounter plasma decomposition by hydrolytic enzymes in the blood and are carried into the liver where they face diverse hepatic metabolic reactions such as phase I oxidations by CYP and flavin monooxygenases (FMO). Unstable compounds often have high clearance (Cl_{int}) and short half-life ($t_{1/2}$) resulting in poor *in vivo* pharmacokinetics (PK) and unsatisfactory pharmacological performance. The *in vitro* plasma and liver microsomal stability of **4**, **13** and **15** were studied by incubating the compounds in rat serum and rat liver microsomes as well as NADPH cofactor**,** respectively, using previously published methods.[43-44] Diltiazem and propranolol were used as co-assay QC controls for plasma and microsomal stability assays, respectively, to ensure that the assays were operating properly, and that the activity of the plasma

and microsomes were consistent with established criteria. As Table 3 shows, **4**, **13** and **15** are more stable than diltiazem in rat plasma. The results also show that **15** exhibits excellent microsomal stability and is more stable than **4** and **13**, in which the suitable hepatic clearance was predicted. The solution stability of **15** was evaluated at pH 5.0, 7.4 and 9.4, respectively.[45] The results indicate that **15** is relatively stable in pH ranging from 5.0 to 9.4 (Table 3).

[Table 3]

The *in vitro* pharmacological studies reveal that compound **15** has many CNS drug-like properties, including appropriate mGluR4 affinity, potent mGluR4 PAM activity and selectivity against other mGluRs, and suitable lipophilicity as well as PPB, adequate metabolic stability and solution stability. Based on these results, compound **15** was selected for radiolabeling and *in vivo* evaluation as a potential mGluR4 PET radioligand.

Radiochemistry. As shown in Scheme 2 the radiolabeling of [^{18}F]**15** was carried out in two steps: 1) generation of [^{18}F]fluoromethyl-d_2 4-methylbenzenesulfonate [^{18}F]**17** by [^{18}F]fluorination of methylene-d_2 bis(4-methylbenzenesulfonate) **16**; 2) the radiolabeling of the thiophenol precursor **18** with [^{18}F]**17**.

[Scheme 2]

Compound [^{18}F]**17** was prepared from the reaction of **16** in acetonitrile and *t*-butanol with non-carrier-added (nca) [^{18}F]fluoride in the presence of tetrabutylammonium bicarbonate at 85 °C for 10 min. The radioactive product was a mixture of [^{18}F]**17** and the side product [^{18}F]**19**, which was purified by semi-preparative HPLC, eluting with a solution of water and acetonitrile (50:50) at a

flow rate of 4 mL/min to give [^{18}F]**17** in 20% yield. The obtained [^{18}F]**17** reacted with the thiophenol precursor **18** in DMSO at 150 ˚C for 10 min, resulting the desired product [^{18}F]**15** in over 95% conversion. The radiolabeled product was purified by semi-preparative HPLC, eluting with 0.1% formic acid solution of water and acetonitrile (40:60) at a flow rate of 4 mL/min to produce [^{18}F]**15**. The final product was obtained after eluting 0.5 mL of ethanol followed by 4.5 mL of sterile saline through the C_{18} Sep-Pak column resulting the final formulation of [^{18}F]**15** in saline containing 10% ethanol with 11.6% ± 2.9% radiochemical yield (RCY, n = 7, decay corrected) and over 99% radiochemical purity. The total synthesis of [^{18}F]**15** took 2.5-3.5 h with the molar activity 84.1 ± 11.8 GBq/μmol (n = 7).

***Ex vivo* Biodistribution Studies.** *Ex vivo* biodistribution studies were carried out in normal male Sprague Dawley rats to quantify accumulation of the tracer in different organs, as well as determine metabolic pathways. These studies showed reversible binding of [^{18}F]**15** in all investigated tissues with maximum uptake between 10 and 20 min except in the kidneys, where excretion of urine can affect tissue activity samples. Liver had the highest accumulation of 1.33±0.12 % ID/g at 20 min followed by kidneys 0.93±0.57 % ID/g at 30 min, lungs 0.58±0.17 % ID/g at 20 min, heart 0.50±0.08 % ID/g at 20 min and brain 0.41±0.18 % ID/g at 10 min. (Figure 4).

[Figure 4]

PET imaging. For *in vivo* characterization with PET imaging, [^{18}F]**15** was synthesized nine times and 30 studies were conducted in male Sprague−Dawley rats comprising 15 baseline studies and 9 blocking studies by using **13** as a blocking agent with doses of 1, 2 or 3 mg/kg and 6 self-blocking studies by using "cold" **15** as blocking agent with the same doses as **13**. These studies demonstrate that [^{18}F]**15** crosses BBB and accumulates in the brain areas known to express mGluR4 (Figure

5). Time-activity curves (TACs) show fast reversible binding in the striatum, thalamus, cerebellum and cortex (Figure 6). The maximum average uptake at the time interval of 1-10 min after administering of the ligand was in the thalamus, 1.77±0.26 % ID/cc. The binding of [^{18}F]**15** in the rat brain was blocked in the whole brain (22-25%) by using **13** and even dose dependently in specific brain areas like striatum, 18, 20 and 28% using doses of 1, 2 or 3 mg/kg. Self-blocking with the same doses of **15** had similar blocking effect with the dose of 2 mg/kg but was significantly lower with 1 mg/kg and higher with 3 mg/kg compared to blocking with **13** (Figure 7). This PET tracer will be further developed in preclinical research with an aim for translational studies.

[Figure 5]

[Figure 6]

[Figure 7]

SUMMARY

In this study, we have designed, synthesized and characterized a new fluorine-18 labeled PET ligand for imaging mGluR4 in the brain. This radioligand displays CNS drug-like properties, including good mGluR4 affinity, potent mGluR4 PAM activity and selectivity against other mGluRs, suitable lipophilicity as well as PPB, adequate metabolic and solution stability. The radiolabeling of [^{18}F]**15** was carried out in two steps. The PET imaging studies in male Sprague−Dawley rats demonstrate that [^{18}F]**15** crosses BBB and accumulates the brain areas known to express mGluR4. Pretreatment with the unlabeled compounds **13** and **15** show the

significant dose-dependent blocking effects. The results suggest that [^{18}F]**15** is a promising candidate for PET imaging of mGluR4 in the brain and for translational studies in PD and/or other disorders.

EXPERIMENTAL SECTION

Animal procedures. The animal studies were approved and done under strict supervision of Subcommittee on Research Animals of the Massachusetts General Hospital and Harvard Medical School and performed in accordance with the Guide of NIH for the Care and Use of Laboratory Animals.

Materials and Methods. All reagents and starting materials were obtained from the commercial sources including Sigma-Aldrich (St. Louis, MO), Thermo Fisher Scientific, Oakwood Products, Inc., Matrix Scientific and used as received. The reactions were monitored by TLC using a UV lamp monitored at 254 nm. If necessary, the reactions were also checked by LC−MS using the Agilent 1200 series HPLC system coupled with a multiwavelength UV detector and a model 6310 ion trap mass spectrometer (Santa Clara, CA) equipped with a Luna C_{18} column (Phenomenex, 100 × 2 mm, 5 μ, 100 Å). The RP-HPLC was carried out by using a 7-min gradient method (LC-Method 1): eluent A: 0.1% formic acid/ H_2O; eluent B: 0.1% formic acid/CH_3CN; gradient: 5% B to 95% B from 0 to 3 min, 95% B from 3 to 4.5 min, 95% to 5% B from 4.5 to 5 min, 5% B from 5 to 7 min; flow rate at 0.7 mL/min. The silica gel used in flash column chromatography was from Aldrich (Cat. 60737, pore size 60 Å, 230-400 mesh). The products were identified by LC−MS as well as ^{1}H NMR, ^{13}C NMR and ^{19}F NMR using a Varian 500 MHz spectrometer. All NMR samples were dissolved in chloroform-*d* ($CDCl_3$) containing tetramethylsilane as a reference standard. Chemical shifts were expressed as ppm and calculated downfield or upfield from the NMR signal

of reference standard. *J* was expressed as Hz, and its splitting patterns were reported as s, d, t, q, or m. HRMS was acquired using a DART-SVP ion source (IonSense, Saugus, MA) attached to a JEOL AccuTOF 4G LC-plus mass spectrometer (JEOLUSA,Peabody, MA) in positive-ion mode from Prof. Peter Caravan's Laboratory. Unless otherwise specified, the purity of all new compounds was over 95% determined by HPLC.

Chemistry. *Fluoromethyl-d_2 4-methylbenzenesulfonate (**17**).* To the solution of methylene-d_2 bis(tosylate) (**16**, 9.01g, 25.2 mmol) in *tert*-amyl alchol (150.0 mL) was added CsF (3.83 g, 25.2 mmol). The mixture was stirred at 80 ˚C for 2.0 h. A large amount of white solid precipitated out. After filtration, the filtrate was condensed under vacuum. The resulting residue was chromatographed on silica gel by eluting with ethyl acetate and hexane (1:30 to 1:15) to afford **17** as a colorless oil (2.49 g, 48%) and 3.02 g of starting material **16** was recovered. ^{1}H NMR (500 MHz, $CDCl_3$) δ 7.83 (d, J = 8.0 Hz, 2H), 7.36 (d, J = 8.0 Hz, 2H), 2.46 (s, 3H). ^{13}C NMR (126 MHz, $CDCl_3$) δ 145.6, 133.8, 129.9 (2C), 127.9 (2C), 97.6 (dp, J = 26.5 Hz, J = 229.3 Hz), 21.7. ^{19}F NMR (470 MHz, $CDCl_3$) δ -154.5 (p, J = 9.4 Hz). LC-MS (method 1): t_R = 3.67 min, (ESI) m/z calcd. for $C_8H_{22}D_2FNO_3S$ 224.0; found 224.0 $[M + NH_4]^+$.

*N-(4-Chloro-3-((fluoromethyl-d_2)thio)phenyl)picolinamide (**15**).* To the solution of *N*-(4-chloro-3-mercaptophenyl)picolinamide hydrogen chloride salt (**18**, 150.0 mg, 0.5 mmol) and **17** (154.5 mg, 0.75 mmol) in acetonitrile (7.0 mL) were added K_2CO_3 (690 mg, 5.0 mmol) and KI (83.0 mg, 0.5 mmol). The resulting mixture was heated to reflux for 2 h. The solvent was removed under vacuum and the residue was dissolved in DCM (20 mL) and water (20 mL). The water phase was further washed with DCM twice (20 mL). The organic layer was combined, dried over anhydrous Na_2SO_4 and concentrated under vacuum. The residue was chromatographed on silica gel by eluting with EtOAc and hexane (1:3) to afford the title product as a white powder (137.2 mg, 92%). ^{1}H

NMR (500 MHz, $CDCl_3$) δ 10.08 (s, 1H), 8.62 (ddd, J = 4.7, 1.6, 0.9 Hz, 1H), 8.29 (dt, J = 7.8, 1.0 Hz, 1H), 7.92 (td, J = 7.7, 1.7 Hz, 1H), 7.86 (d, J = 1.7 Hz, 1H), 7.51 (ddd, J = 7.6, 4.7, 1.2 Hz, 1H), 7.44 (dd, J = 8.7, 2.3 Hz, 1H), 7.39 (d, J = 8.6 Hz, 1H). ^{19}F NMR (470 MHz, $CDCl_3$) δ -150.9 (dt, J = 16.2, 8.2 Hz). ^{13}C NMR (126 MHz, $CDCl_3$) δ 162.1, 149.3, 148.0, 137.8, 137.3, 134.3, 130.2, 128.62 (d, J = 2.4 Hz), 126.7, 122.5, 120.6, 119.5, 85.8 (dp, J = 24.0, 217.2 Hz). LC-MS (method A1): t_R = 4.05 min, (ESI) m/z calcd. for $C_{13}H_9D_2ClFN_2OS$ 299.0; found 298.9 [M + H]$^+$. HRMS (m/z) calcd. for $C_{13}H_9D_2ClFN_2OS$ 299.0390; found 299.0388 [M + H]$^+$.

Radiochemistry Procedure. [^{18}F]Fluoride was generated by a Siemens Eclipse HP 11 MeV cyclotron (Malvern, PA) using ^{18}O-enriched water (Isoflex Isotope, San Francisco, CA) with proton bombardment. Fluorine-18 labeling of [^{18}F]**15** was accomplished in two steps. First, [^{18}F]fluoride in ^{18}O-enriched water was passed through a QMA Sep-Pak Cartridge (Waters, Milford, MA) to trap [^{18}F]fluoride ions, which was washed off by 0.5 mL of the aqueous solution of tetrabutylammonium hydrogen carbonate (75 mM, from ABX advanced biochemical compounds). Acetonitrile (1.0 mL) was added to the solution and the solvents were evaporated at 115 °C in a stream of nitrogen. In order to remove water completely, 1.0 mL of acetonitrile was added and evaporated in a stream of nitrogen three more times. To the residue containing [^{18}F]fluoride was added **16** (12.0 mg) in 0.7 mL of acetonitrile and *t*-BuOH (4:1). The resulting solution was heated to 85 °C for 10 min and then cooled to room temperature followed by addition of 1.5 mL of water. The mixture was then purified by a semi-preparative HPLC (Waters 4000 system equipped with an Xbridge BEH C_{18} OBD column: 130 Å, 5 μ, 10 × 250 mm) by eluting with a solution of water and acetonitrile (50:50) at a flow rate of 4 mL/min to give the fractions containing [^{18}F]**17**. The combined fraction was diluted with water to 40 mL and loaded on a C_{18} Sep-Pak column. The column was further dried through a stream of nitrogen for 20-30 min. [^{18}F]**17**

was washed off the C_{18} Sep-Pak column by 0.7 mL of dry DMSO to a reaction vessel containing 2.0 mg of **18** and cesium carbonate (3.0 - 5.0 mg). The resulting mixture was heated to 150 ˚C for 10 min and then cooled to rt, followed by addition of the HPLC eluents (2.5 mL, 0.1% formic acid solution of water and acetonitrile 40:60). The mixture was then purified using the semi-preparative HPLC (Waters 4000 system equipped with an Xbridge BEH C_{18} OBD column: 130 Å, 5 μ, 250 × 10 mm) by eluting with a 0.1% formic acid solution of water and acetonitrile (40:60) at a flow rate of 4 mL/min. The fraction containing [^{18}F]**15** was diluted with water to 40 mL and loaded on a C_{18} Sep-Pak column to give the final formulation of [^{18}F]**15** in saline containing 10% ethanol with 11.6% ± 2.9% radiochemical yield (RCY, n = 7, decay corrected). The purity of [^{18}F]**15** was over 99% that was analyzed by an analytical HPLC (Waters 2487 series equipped with a UV detector and a BIOSCAN radioactivity detector and an ACE 5 C_{18}-AR column: 250 × 10 mm, 5 μ). Identity of [^{18}F]**15** was confirmed by co-injection of the cold compound **15** in HPLC analysis. The total synthesis of [^{18}F]**15** took 2.5-3.5 h with the molar activity 84.1 ± 11.8 GBq/μmol (n =7).

Determination of Log D. An aliquot (10 μL, 74 kBq) of [^{18}F]**15** was added to a test tube containing 2.5 mL of octanol and 2.5 mL of phosphate buffer solution (pH 7.4). The test tube was mixed by vortex for 2 min and then centrifuged for 2 min to fully separate the aqueous and organic phase. The samples taken from the octanol layer (0.1 mL) and the aqueous layer (1.0 mL) were saved for radioactivity measurement. An additional aliquot of the octanol layer (2.0 mL) was carefully transferred to a new test tube containing 0.5 mL of octanol and 2.5 mL of phosphate buffer solution (pH 7.4). The previous procedure (vortex mixing, centrifugation, sampling, and transfer to the next test tube) was repeated until six sets of aliquot samples had been prepared. The radioactivity of each sample was measured using PerkinElmer Wizard2 2480 gamma-counter. The log D of each set of samples was calculated as the following:

Log $D_{7.4}$ = Log (radioactivity of octanol layer × 10 / radioactivity of PBS layer)

Plasma Protein Binding Assay. An aliquot of radiolabeled compound [^{18}F]**15** in saline (10 μL, 74 kBq) was added to a sample of human plasma (0.5 mL). The mixture was gently mixed by repeated inversion and incubated for 10 min at room temperature. Following incubation, a small sample (10 μL) was removed to determine the total radioactivity in the plasma sample (A_T; $A_T = A_{bound} + A_{unbound}$). The upper part of the Centrifree tube was discarded, and an aliquot (10 μL) from the bottom part of the tube was removed to determine the amount of unbound radioactivity ($A_{unbound}$) that passed through the membrane **(**molecular weight cutoff 30 kD). The radioactivity of each sample was measured using PerkinElmer Wizard2 2480 gamma-counter. Plasma protein binding was derived by the following equation: %unbound= $A_{unbound}$ x 100/A_T.

***Ex vivo* Studies of Biodistribution.** For biodistribution studies the normal male Sprague Dawley rats were anesthetized with isoflurane/nitrous oxide (1-1.5% isoflurane) to install catheter into the tail vain for administration of radioactivity ([^{18}F]**15,** 22±3 MBq, iv, mass 0.072±0.09 μg). Total of 15 rats in deep anesthesia (isoflurane 4% and cervical dislocation) were sacrificed in a group of three at five different time points (5, 10, 20, 30, and 60 min) after injection of [^{18}F]**15**. Major organs including lung, heart, liver, spleen, kidney, muscle, midbrain, cortex, cerebellum and blood were harvested to determine radioactivity. The tissue samples were weighted, and the radioactivity was measured with the standard samples of [^{18}F]**15** using Wizard2 2480, Perkin Elmer, CA. Radioactivity of the tissue samples was determined as percent of the injected activity per gram of the tissue.

PET Imaging of [^{18}F]15 in Rats. Altogether 24 normal male Sprague Dawley rats were used for the imaging studies comprising 15 baseline studies and 15 blocking studies. Rats were anaesthetized with isoflurane/nitrous oxide (1.0-1.5% isoflurane, with oxygen flow of 1-1.5 L/min),

and catheter was installed into tail vein for the administration of [^{18}F]**15**. Dynamic volumetric PET data was acquired with a PET-CT scanner for 60 min (Triumph-II, Tri-Foil Imaging, Northridge, CA). The vital signals such as heart rate and respiration rate were monitored during scanning period. PET data acquisition was started immediately after administration of radioactivity with the dose range of 18-34 MBq (mass 0.059±0.111 µg) depending on the size of the rat followed by CT imaging to obtain anatomical information and data for attenuation correction of PET data. PET data was processed by using maximum-likelihood expectation-maximization (MLEM) algorithm with 30 iterations to dynamic volumetric images, and corrected for uniformity, scatter, and attenuation. The CT data was processed by the modified Feldkamp algorithm using matrix volumes of 512×512×512 and pixel size of 170 µm. Co-registration of CT and PET images and analysis of PET images were carried out using PMOD3.2 software (PMOD Technology, Zurich, Switzerland).

For blocking studies, the same scanning protocols were used as for the baseline studies. For mGluR4 blocking experiments, 1, 2 or 3 mg/kg of **13** or **15** dissolved in a saline solution with 10% DMSO, 5% Tween-20 and 85% PBS was injected 1 min before iv administration of [^{18}F]**15**.

ASSOCIATED CONTENT

Supporting Information

The *in vitro* assays including the radioligand replacement assay, the mGluR functional assays and metabolic as well as solution stability assays are described in the Supporting Information that is available free of charge on the ACS Publications website at DOI:

AUTHOR INFORMATION

Corresponding Authors

*A-L.B.: phone, 617-744-3725; e-mail: abrownell@mgh.harvard.edu

*Z.Z.: phone, 617-643-4887; e-mail: zzhang9@mgh.harvard.edu

Author Contributions

The manuscript was written through contributions of all authors. All authors have given approval to the final version of the manuscript.

Notes

The authors declare no competing financial interest.

ACKNOWLEDGMENTS

The authors would like to acknowledge supporting research grants R01NS10064, R01EB021708 and R01EB012864 and the grants 1S10RR023452-01 and 1S10OD025234-01 for the imaging instrumentation and characterization of the organic compounds. As well the authors like to thank the technical staffs at the cyclotron facility at Massachusetts General Hospital.

mGluR1-6 and mGluR8 agonist and antagonist functional data as well as mGluR4 PAM activity were generously provided by the National Institute of Mental Health's Psychoactive Drug

Screening Program, Contract # HHSN-271-2013-00017-C (NIMH PDSP). The NIMH PDSP is Directed by Bryan L. Roth (mailto:bryan_roth@med.unc.edu) at the University of North Carolina at Chapel Hill and Project Officer Jamie Driscoll (mailto:jdrisco1@mail.nih.gov) at NIMH, Bethesda MD, USA. For experimental details please refer to the PDSP web site https://pdspdb.unc.edu/pdspWeb/ (https://pdspdb.unc.edu/pdspWeb/).

ABBREVIATIONS USED

Cl_{int}, the intrinsic clearance; G_i, adenylate cyclase inhibitory G-protein; L-SOP, L-Serine-O-phosphate; TAC, time-activity curve; %ID/g, percentage of injected dose per gram of wet tissue.

REFERENCES

1. Dauer, W.; Przedborski, S., Parkinson's disease: Mechanisms and models. *Neuron* **2003,** *39*, 889-909.

2. De Rijk, M. C.; Launer, L. J.; Berger, K.; Breteler, M. M.; Dartigues, J. F.; Baldereschi, M.; Fratiglioni, L.; Lobo, A.; Martinez-Lage, J.; Trenkwalder, C.; Hofman, A., Prevalence of Parkinson's disease in Europe: A collaborative study of population-based cohorts. Neurologic Diseases in the Elderly Research Group. *Neurology* **2000,** *54*, S21-23.

3. Masilamoni, G. J.; Smith, Y., Metabotropic glutamate receptors: targets for neuroprotective therapies in Parkinson disease. *Curr. Opin. Pharmacol.* **2018,** *38*, 72-80.

4. DeLong Mahlon, R.; Wichmann, T., Basal Ganglia Circuits as Targets for Neuromodulation in Parkinson Disease. *JAMA Neurol* **2015,** *72*, 1354-1360.

5. Sebastianutto, I.; Cenci, M. A., mGlu receptors in the treatment of Parkinson's disease and L-DOPA-induced dyskinesia. *Curr. Opin. Pharmacol.* **2018,** *38*, 81-89.

6. Charvin, D., mGlu4 allosteric modulation for treating Parkinson's disease. *Neuropharmacology* **2018,** *135*, 308-315.

7. Mellone, M.; Gardoni, F., Glutamatergic mechanisms in L-DOPA-induced dyskinesia and therapeutic implications. *J. Neural Transm.* **2018,** *125*, 1225-1236.

8. Amalric, M.; Lopez, S.; Goudet, C.; Fisone, G.; Battaglia, G.; Nicoletti, F.; Pin, J. P.; Acher, F. C., Group III and subtype 4 metabotropic glutamate receptor agonists: Discovery and pathophysiological applications in Parkinson's disease. *Neuropharmacology* **2013,** *66*, 53-64.

9. Huang, X.; Dale, E.; Brodbeck, R. M.; Doller, D., Chemical Biology of mGlu4 Receptor Activation: Dogmas, Challenges, Strategies and Opportunities. *Curr. Top. Med. Chem. (Sharjah, United Arab Emirates)* **2014,** *14*, 1755-1770.

10. Conn, P. J. P., J. P., Pharmacology and functions of metabotropic glutamate receptors. *Ann. Rev. Pharmacol. Toxicol.* **1997,** *37*, 205-237.

11. Corti, C.; Aldegheri, L.; Somogyi, P.; Ferraguti, F., Distribution and synaptic localisation of the metabotropic glutamate receptor 4 (mGluR4) in the rodent CNS. *Neuroscience (Oxford, U. K.)* **2002,** *110*, 403-420.

12. Valenti, O. M., G.; Seabrook, G. R.; Conn, P. J.; Marino, M. J., Group III metabotropic glutamate-receptor-mediated modulation of excitatory transmission in rodent substantia nigra pars compacta dopamine neurons. *Journal of Pharmcology and Experimental Therapeutics* **2005,** *313*, 1296-1304.

13. Niswender, C. M.; Conn, P. J., Metabotropic glutamate receptors: physiology, pharmacology, and disease. *Ann. Rev. Pharmacol. Toxicol.* **2010,** *50*, 295-322.

14. Goudet, C.; Vilar, B.; Courtiol, T.; Deltheil, T.; Bessiron, T.; Brabet, I.; Oueslati, N.; Rigault, D.; Bertrand, H.-O.; McLean, H.; Daniel, H.; Amalric, M.; Acher, F.; Pin, J.-P., A novel selective metabotropic glutamate receptor 4 agonist reveals new possibilities for developing subtype selective ligands with therapeutic potential. *Faseb J* **2012,** *26*, 1682-1693.

15. Cajina, M.; Nattini, M.; Song, D.; Smagin, G.; Joergensen, E. B.; Chandrasena, G.; Bundgaard, C.; Toft, D. B.; Huang, X.; Acher, F.; Doller, D., Qualification of LSP1-2111 as a Brain Penetrant Group III Metabotropic Glutamate Receptor Orthosteric Agonist. *ACS Med. Chem. Lett.* **2014,** *5*, 119-123.

16. Lindsley, C. W.; Hopkins, C. R., Metabotropic glutamate receptor 4 (mGlu4)-positive allosteric modulators for the treatment of Parkinson's disease: historical perspective and review of the patent literature. *Expert Opin. Ther. Pat.* **2012,** *22*, 461-481.

17. Robichaud, A. J. E., D. W.; Lindsley, C. W.; Hopkins, C. R., Recent progress on the identification of metabotropic glutamate 4 receptor ligands and their potential utility as CNS therapeutics. *ACS Chem. Neurosci.* **2011,** *17*, 433-449.

18. Marino, M. J.; Williams, D. L., Jr.; O'Brien, J. A.; Valenti, O.; McDonald, T. P.; Clements, M. K.; Wang, R.; DiLella, A. G.; Hess, J. F.; Kinney, G. G.; Conn, P. J., Allosteric modulation of group III metabotropic glutamate receptor 4: A potential approach to Parkinson's disease treatment. *Proc. Natl. Acad. Sci. U. S. A.* **2003,** *100*, 13668-13673.

19. Battaglia, G.; Busceti, C. L.; Molinaro, G.; Biagioni, F.; Traficante, A.; Nicoletti, F.; Bruno, V., Pharmacological activation of mGlu4 metabotropic glutamate receptors reduces

nigrostriatal degeneration in mice treated with 1-methyl-4-phenyl-1,2,3,6-tetrahydropyridine. *J. Neurosci.* **2006,** *26*, 7222-7229.

20. Charvin, D.; Pomel, V.; Ortiz, M.; Frauli, M.; Scheffler, S.; Steinberg, E.; Baron, L.; Deshons, L.; Rudigier, R.; Thiarc, D.; Morice, C.; Manteau, B.; Mayer, S.; Graham, D.; Giethlen, B.; Brugger, N.; Hedou, G.; Conquet, F.; Schann, S., Discovery, Structure-Activity Relationship, and Antiparkinsonian Effect of a Potent and Brain-Penetrant Chemical Series of Positive Allosteric Modulators of Metabotropic Glutamate Receptor 4. *J. Med. Chem.* **2017,** *60*, 8515-8537.

21. Le Poul, E.; Bolea, C.; Girard, F.; Poli, S.; Charvin, D.; Campo, B.; Bortoli, J.; Bessif, A.; Luo, B.; Koser, A. J.; Hodge, L. M.; Smith, K. M.; DiLella, A. G.; Liverton, N.; Hess, F.; Browne, S. E.; Reynolds, I. J., A potent and selective metabotropic glutamate receptor 4 positive allosteric modulator improves movement in rodent models of Parkinson's disease. *J. Pharmacol. Exp. Ther.* **2012,** *343*, 167-177.

22. Jones, C. K.; Bubser, M.; Thompson, A. D.; Dickerson, J. W.; Turle-Lorenzo, N.; Amalric, M.; Blobaum, A. L.; Bridges, T. M.; Morrison, R. D.; Jadhav, S.; Engers, D. W.; Italiano, K.; Bode, J.; Daniels, J. S.; Lindsley, C. W.; Hopkins, C. R.; Conn, P. J.; Niswender, C. M., The metabotropic glutamate receptor 4-positive allosteric modulator VU0364770 produces efficacy alone and in combination with L-DOPA or an adenosine 2A antagonist in preclinical rodent models of Parkinson's disease. *J. Pharmacol. Exp. Ther.* **2012,** *340*, 404-421.

23. Niswender, C. M.; Johnson, K. A.; Weaver, C. D.; Jones, C. K.; Xiang, Z.; Luo, Q.; Rodriguez, A. L.; Marlo, J. E.; de Paulis, T.; Thompson, A. D.; Days, E. L.; Nalywajko, T.; Austin, C. A.; Williams, M. B.; Ayala, J. E.; Williams, R.; Lindsley, C. W.; Conn, P. J., Discovery,

characterization, and antiparkinsonian effect of novel positive allosteric modulators of metabotropic glutamate receptor 4. *Mol. Pharmacol.* **2008,** *74*, 1345-1358.

24. Niswender, C. M.; Jones, C. K.; Lin, X.; Bubser, M.; Thompson Gray, A.; Blobaum, A. L.; Engers, D. W.; Rodriguez, A. L.; Loch, M. T.; Daniels, J. S.; Lindsley, C. W.; Hopkins, C. R.; Javitch, J. A.; Conn, P. J., Development and Antiparkinsonian Activity of VU0418506, a Selective Positive Allosteric Modulator of Metabotropic Glutamate Receptor 4 Homomers without Activity at mGlu2/4 Heteromers. *ACS Chem. Neurosci.* **2016,** *7*, 1201-1211.

25. Bennouar, K.-E.; Uberti, M. A.; Melon, C.; Bacolod, M. D.; Jimenez, H. N.; Cajina, M.; Kerkerian-Le Goff, L.; Doller, D.; Gubellini, P., Synergy between L-DOPA and a novel positive allosteric modulator of metabotropic glutamate receptor 4: Implications for Parkinson's disease treatment and dyskinesia. *Neuropharmacology* **2013,** *66*, 158-169.

26. Broadstock, M.; Austin, P. J.; Betts, M. J.; Duty, S., Antiparkinsonian potential of targeting group III metabotropic glutamate receptor subtypes in the rodent substantia nigra pars reticulata. *Br J Pharmacol* **2012,** *165*, 1034-1045.

27. Betts, M. J.; O'Neill, M. J.; Duty, S., Allosteric modulation of the group III mGlu4 receptor provides functional neuroprotection in the 6-hydroxydopamine rat model of Parkinson's disease. *Br. J. Pharmacol.* **2012,** *166*, 2317-2330.

28. Ponnazhagan, R.; Harms Ashley, S.; Thome Aaron, D.; Jurkuvenaite, A.; Standaert David, G.; Gogliotti, R.; Niswender Colleen, M.; Conn, P. J., The Metabotropic Glutamate Receptor 4 Positive Allosteric Modulator ADX88178 Inhibits Inflammatory Responses in Primary Microglia. *J Neuroimmune Pharmacol* **2016,** *11*, 231-237.

29. Zhang, Z.; Brownell, A.-L., Imaging of Metabotropic Glutamate Receptors (mGluR)s. In

Neuroimaging - Clinical applications Bright, P., Ed. InTech - Open Access Publisher: Rijeka, Croatia, 2012; pp 499-532.

30. Kil, K.-E. Z., Z.; Jokivarsi, K.; Gong, C.; Choi, J.-K.; Kura, S.; Brownell, A.-L., Radiosynthesis of N-(4-chloro-3-[^{11}C]methoxyphenyl)-2-picolinamide ([^{11}C]ML128) as a PET radiotracer for metabotropic glutamate receptor subtype 4 ($mGlu_4$). *Bioorganic and Medicinal Chemistry* **2013,** *21*, 5955-5962.

31. Kil, K.-E.; Poutiainen, P.; Zhang, Z.; Zhu, A.; Choi, J.-K.; Jokivarsi, K.; Brownell, A.-L., Radiosynthesis and Evaluation of an 18F-Labeled Positron Emission Tomography (PET) Radioligand for Metabotropic Glutamate Receptor Subtype 4 (mGlu4). *J. Med. Chem.* **2014,** *57*, 9130-9138.

32. Kil, K.-E.; Poutiainen, P.; Zhang, Z.; Zhu, A.; Kuruppu, D.; Prabhakar, S.; Choi, J.-K.; Tannous, B. A.; Brownell, A.-L., Synthesis and evaluation of N-(methylthiophenyl)picolinamide derivatives as PET radioligands for metabotropic glutamate receptor subtype 4. *Bioorg. Med. Chem. Lett.* **2016,** *26*, 133-139.

33. Fujinaga, M.; Yamasaki, T.; Nengaki, N.; Ogawa, M.; Kumata, K.; Shimoda, Y.; Yui, J.; Xie, L.; Zhang, Y.; Kawamura, K.; Zhang, M.-R., Radiosynthesis and evaluation of 5-methyl-N-(4-[11C]methylpyrimidin-2-yl)-4-(1H-pyrazol-4-yl)thiazol-2-amine ([11C]ADX88178) as a novel radioligand for imaging of metabotropic glutamate receptor subtype 4 (mGluR4). *Bioorg. Med. Chem. Lett.* **2016,** *26*, 370-374.

34. Takano, A.; Nag, S.; Jia, Z.; Jahan, M.; Forsberg, A.; Arakawa, R.; Grybaeck, P.; Duvey, G.; Halldin, C.; Charvin, D., Characterization of [11C]PXT012253 as a PET Radioligand for mGlu4 Allosteric Modulators in Nonhuman Primates. *Mol. Imaging Biol.* **2019**, *21,* 500-508.

35. Charvin, D.; Di Paolo, T.; Bezard, E.; Gregoire, L.; Takano, A.; Duvey, G.; Pioli, E.; Halldin, C.; Medori, R.; Conquet, F., An mGlu4-Positive Allosteric Modulator Alleviates Parkinsonism in Primates. *Mov. Disord.* **2018,** *33*, 1619-1631.

36. Zhang, Z.; Kil, K.-E.; Poutiainen, P.; Choi, J.-K.; Kang, H.-J.; Huang, X.-P.; Roth, B. L.; Brownell, A.-L., Re-exploring the N-phenylpicolinamide derivatives to develop mGlu4 ligands with improved affinity and in vitro microsomal stability. *Bioorg. Med. Chem. Lett.* **2015,** *25*, 3956-3960.

37. Wang, J.; Shoup, T. M.; Brownell, A.-L.; Zhang, Z., Improved synthesis of the thiophenol precursor N-(4-chloro-3-thiophenyl)picolinamide formaking the mGluR4 PET ligand. *Tetrahedron* **2019,** *75,* 3917-3922**.**

38. Poutiainen, P.; Kil, K.-E.; Zhang, Z.; Kuruppu, D.; Tannous, B.; Brownell, A.-L., Co-operative binding assay for the characterization of mGlu4 allosteric modulators. *Neuropharmacology* **2015,** *97*, 142-148.

39. Roth, B. L., Assay protocol book. Version III ed.; PDSP, N., Ed. Department of Pharmacology, University of North Carolina at Chapel Hill, 2018.

40. DiRaddo, J. O.; Miller, E. J.; Hathaway, H. A.; Grajkowska, E.; Wroblewska, B.; Wolfe, B. B.; Liotta, D. C.; Wroblewski, J. T., A real-time method for measuring cAMP production modulated by Gαi/o-coupled metabotropic glutamate receptors. *J. Pharmacol. Exp. Ther.* **2014,** *349*, 373-382.

41. Pike, V. W., PET radiotracers: crossing the blood-brain barrier and surviving metabolism. *Trends Pharmacol. Sci.* **2009,** *30*, 431-440.

42. Honer, M.; Gobbi, L.; Martarello, L.; Comley, R. A., Radioligand development for molecular imaging of the central nervous system with positron emission tomography. *Drug Discov. Today* **2014,** *19*, 1936-1944.

43. Di, L.; Kerns, E. H.; Hong, Y.; Chen, H., Development and application of high throughput plasma stability assay for drug discovery. *Int. J. Pharmaceutics* **2005,** *297*, 110-119.

44. Houston, J. B., Utility of in vitro drug metabolism data in predicting in vivo metabolic clearance. *Biochem. Pharmacol.* **1994,** *47*, 1469-1479.

45. Di, L.; Kerns, E. H.; Chen, H.; Petusky, S. L., Development and application of an automated solution stability assay for drug discovery. *J. Biomol. Screening* **2006,** *11*, 40-47.

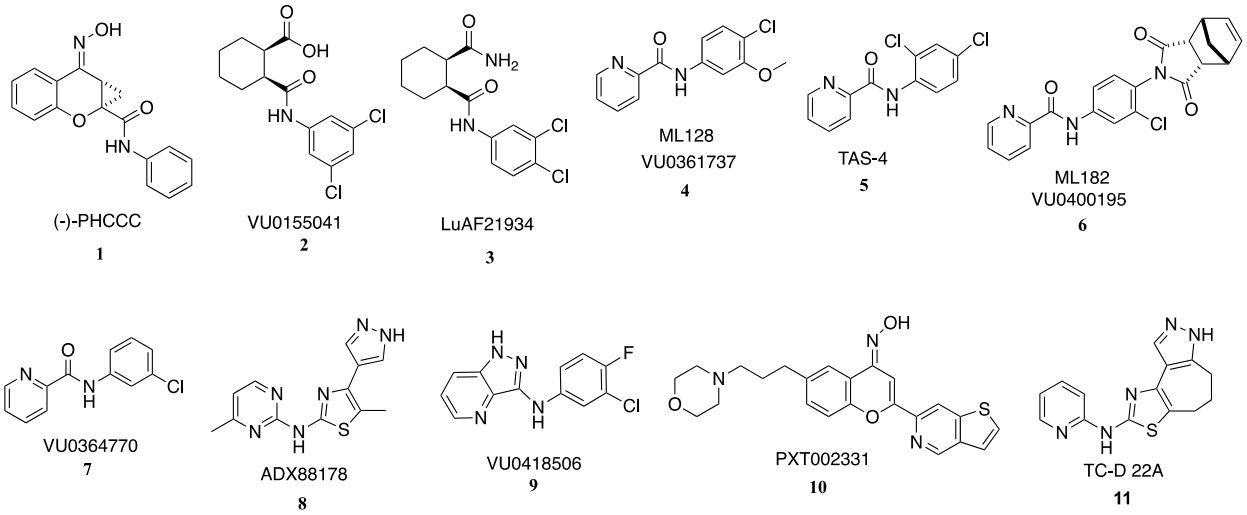

Figure 1. Representative mGluR4 PAMs.

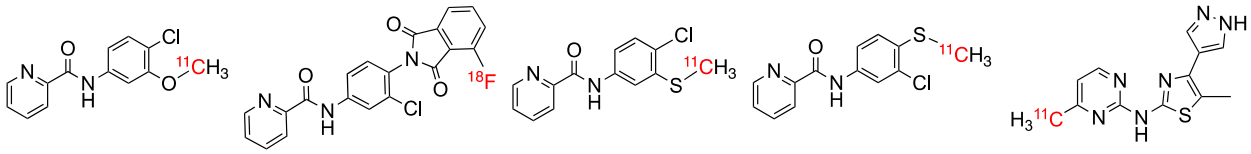

Figure 2. PET tracers for mGluR4. We have previously synthesized and reported the tracers [^{11}C]**4**[31], [^{18}F]**12**[32], [^{11}C]**13**[33] and [^{11}C]**14**[33].

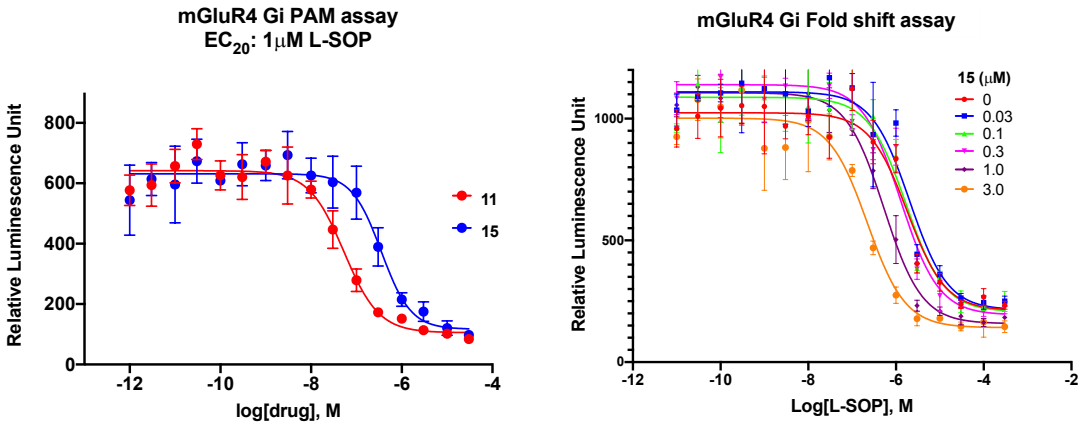

Figure 3. Quantification of the allosteric effects of mGluR4 PAM **15** by using a cAMP assay.

(Left) mGluR4 Gi PAM activity assay, in which mGluR4 PAM (**11** or **15**) potentiates the effect induced by an EC_{20} glutamate concentration (EC_{50}: 324 nM for **15**; 55 nM for **11**);

(Right) mGluR4 Gi fold shift assay, in which **15** shifts the agonist (L-SOP) response curves to the left 7.5-fold at 3.0 μM in 98.3% Glu Max efficacy. Data represents the average of at least three independent determinations performed in triplicate.

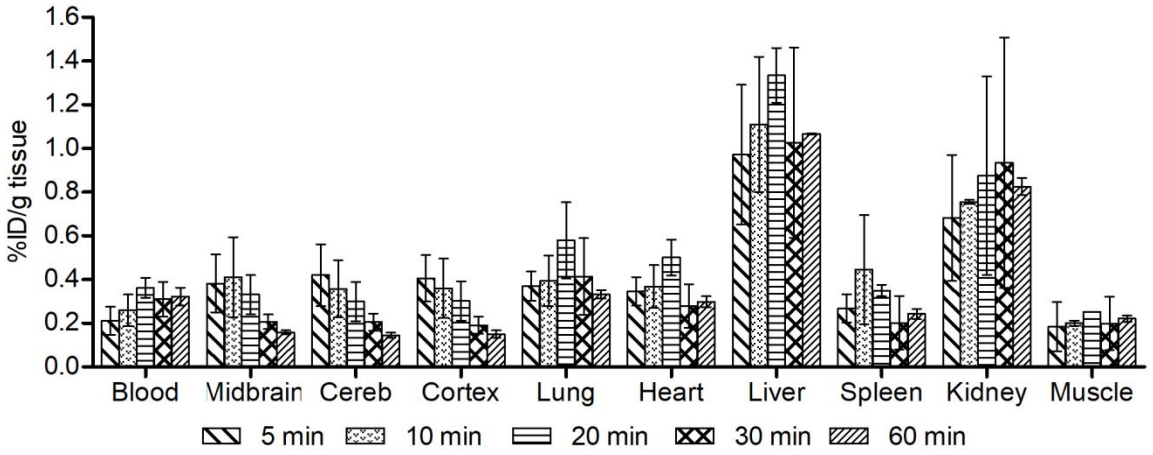

Figure 4. Biodistribution of [^{18}F]**15.**

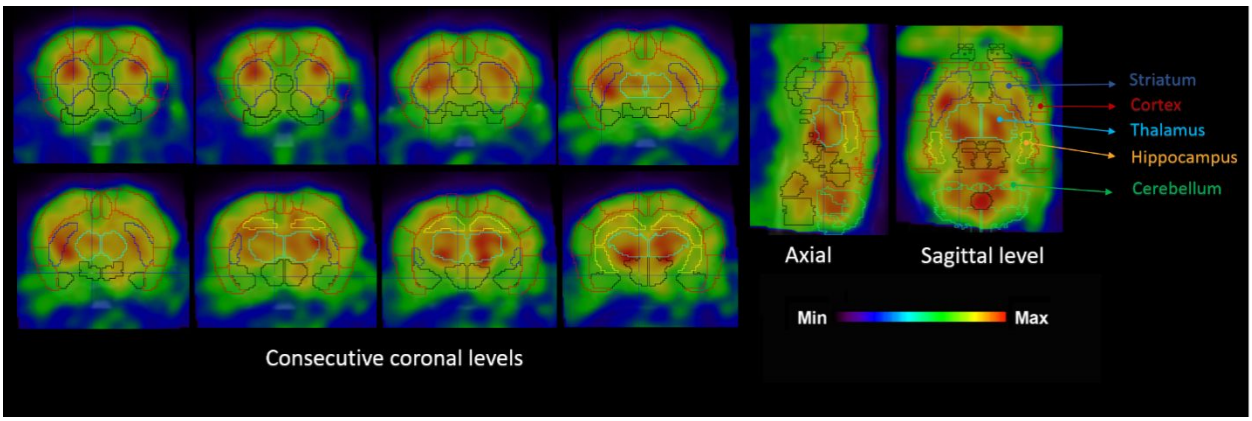

Figure 5. Eight consecutive coronal slices and midbrain axial and sagittal slices fused with the anatomical borderlines of different brain areas show the distribution of [^{18}F]**15** in the rat brain (Sprague Dawley). The images show the average accumulation of [^{18}F]**15** between 1 and 15 min after administration of the radioactivity. Note that the maximum color code refers to the maximum pixel value in each image. The borderlines of different brain areas and their names are color coded to match the corresponding TACS in Figure 6.

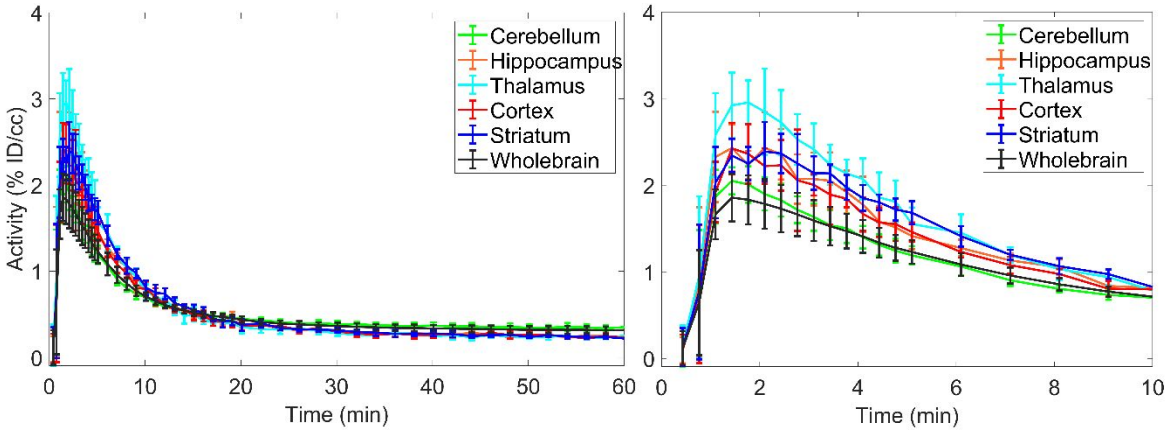

Figure 6. Time-activity curves show fast accumulation and washout in all investigated brain areas. The highest accumulation was observed in the thalamus. The baseline data is averaged from five normal male rats (Sprague Dawley) with weight between 205-225 g. (left) The follow up period of 60 min shows that after 20 min the washout from striatum is low while the cerebellar activity stays nearly constant. (right) Accumulation in the different brain parts can be seen separately during the first 10 min. This image shows the highest accumulation in the thalamus achieved about 2 min after administration of the ligand.

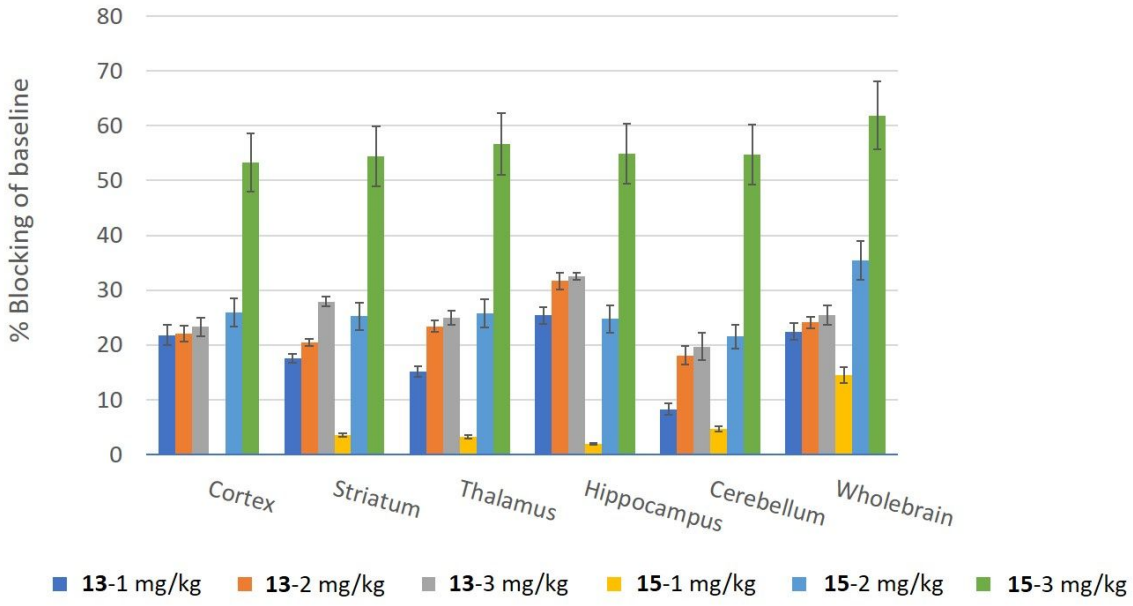

Figure 7. Blocking was calculated as a percent change from the baseline values. Blocking studies show that both **13** and **15** inhibit [^{18}F]**15** binding dose dependently. The blocking effect using **13** with the doses of 1, 2 or 3 mg/kg was from 8 to 32 percent in different brain areas while using **15** it was from 1 to 61 percent from the baseline values. However, the blocking effect with the dose of 2 mg/kg **15** was at the same level as with **13**.

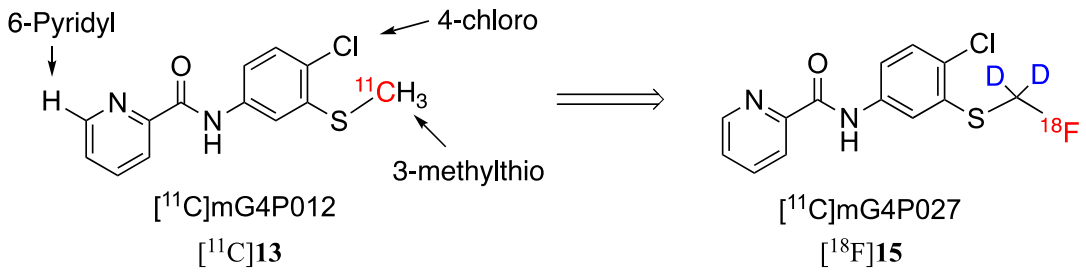

Chart 1. The design of [^{18}F]**15** from the structure of [^{11}C]**13**.

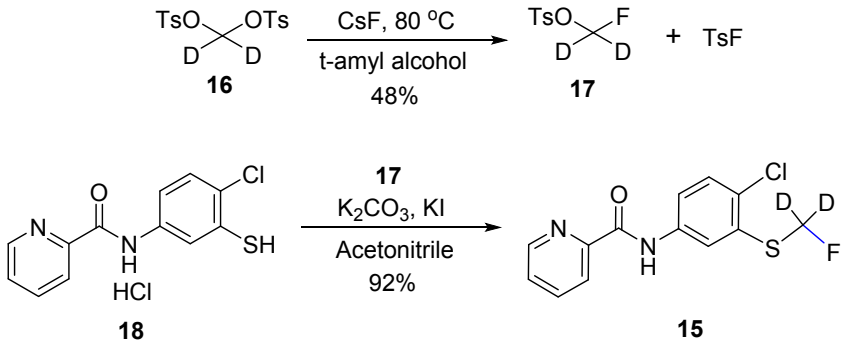

Scheme 1. Synthesis of compound **15**.

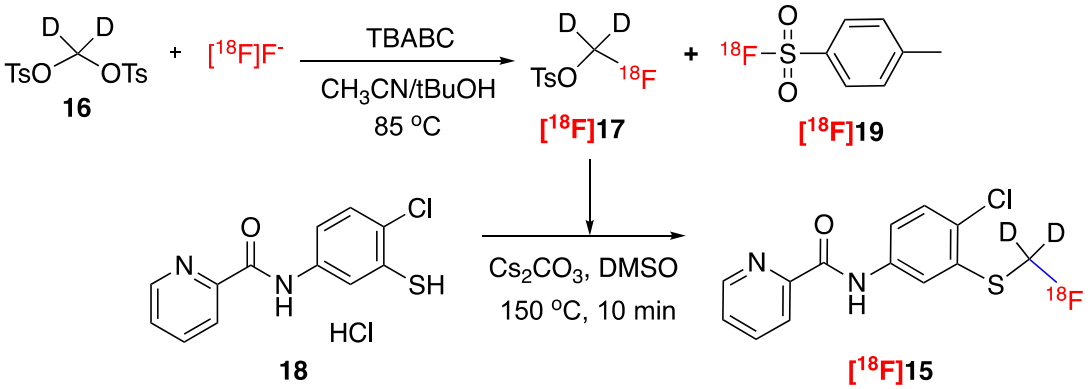

Scheme 2. Radiosynthesis of [^{18}F]**15**.

Table 1. Affinity to mGluR4.

Compound	**4**	**8**	**13**	**15**
IC_{50}±SE (nM)	5.1±1.1	3.2±0.6	3.5±0.7	3.5±0.5
log(IC_{50}±SE)	-8.29±0.09	-8.49±0.07	-8.46±0.08	-8.46±0.06

Table 2. Pharmacochemical properties.

Compound	MW	tPSA	HBD	cLogP	Log $D_{7.4}$	PPB
15	298.76	41.46	1	2.95	3.82	93.1%

Table 3. Metabolic and solution stabilities.

Compound	The plasma stability	The microsome stability		The solution stability		
	The intact ± SEM at 120 min (%)	$t_{1/2}$ (min)	Clint (μL/min /mg protein)	The intact ± SEM at 120 min (%)		
				pH = 5.0	pH = 7.4	pH = 9.4
4	98.2 ± 6.3	14.4	96.2	92.7 ± 3.1	97.3 ± 1.1	89.1 ± 2.1
13	91.5 ± 2.5	25.3	54.8	85.9 ± 0.8	87.9 ± 3.4	89.3 ± 1.3
15	84.5 ± 10.2	57.3	24.2	87.1 ± 0.9	88.3 ± 1.9	84.3 ± 1.8
Diltiazem	49.0 ± 10.6	--	--	94.7 ± 1.4	99.0 ± 5.7	69.8 ± 2.6
Propranolol	--	3.6	390	--	--	--

Table of Contents Graphic